High-spin states in ^{205}At

T. P. Sjoreen,* D. B. Fossan, U. Garg,† A. Neskakis,‡ A. R. Poletti§
Department of Physics, State University of New York, Stony Brook, New York 11794

E. K. Warburton
Department of Physics, Brookhaven National Laboratory, Upton, New York 11793
(Received 9 July 1981)

The properties of high-spin states in ^{205}At have been studied with the ^{197}Au (^{12}C, $4n$) ^{205}At reaction. In-beam measurements [with Ge(Li) detectors] of γ-γ coincidences, γ-ray angular distributions, and pulsed-beam γ timing were made to determine the decay scheme, level energies, γ-ray multipolarities, spin-parity assignments, and isomeric lifetimes. High-spin states up to $29/2\,\hbar$ were identified as either proton excitations of the ($N=126$) ^{211}At nucleus coupled to the ^{202}Pb ($Z=82$) ground state or neutron excitations of ^{202}Pb coupled to the $(\pi h_{9/2})^3 \frac{9}{2}^-$ ground state of ^{211}At. The lifetime measurements of the $\frac{25}{2}^+$ 2062-keV state and the unobserved isomeric state ($\frac{29}{2}^+$) above 2339 keV yielded mean lifetimes of 92(3) nsec and ~ 3 μsec, respectively.

[NUCLEAR REACTIONS ^{197}Au (^{12}C, $4n\gamma$)^{205}At, $E_{^{12}C}=77$ MeV, measured γ-γ coincidence, γ-$W(\theta)$, pulsed-beam γ timing; deduced levels, γ multipolarities, J^π, $T_{1/2}$, $B(E1)$.]

I. INTRODUCTION

Recently, the odd-proton ^{207,209,213}At isotopes ($Z=85$) have been studied at Stony Brook[1–3] using the ^{204,206}Pb (^{6}Li, $3n$) ^{207,209}At and ^{208}Pb(^{7}Li, $2n$) ^{213}At reactions along with in-beam γ-ray spectroscopy. The purpose of these measurements was to investigate the interaction between the valence three-proton structure (π^3) defined by the closed neutron shell ($N=126$) nucleus ^{211}At (Ref. 4) and the neutron excitations $(\nu)^n$ of the corresponding even Pb nuclei[5] ($Z=82$). The experiments were successful in showing that the observed low-lying high-spin states ($\frac{9}{2} \leq J \leq \frac{29}{2}$) could be interpreted in weak coupling as ^{211}At configurations involving the $h_{9/2}$, $f_{7/2}$, and $i_{13/2}$ orbitals coupled to the appropriate Pb core configurations.

In the present paper these studies have been extended to ^{205}At to determine the extent to which the six neutron hole structure of ^{202}Pb influences the ^{205}At level scheme and to search for the onset of collectivity for specific proton configurations. At the beginning of the present investigation, the only available information on ^{205}At came from a study[6] of low-spin states via the β decay of ^{205}Rn and a study[7] of high-spin states using the ^{197}Au(^{12}C,$4n$) reaction. The results of this (^{12}C,$4n$) study provided an additional motivation for the present work because the deduced ^{205}At level scheme, obtained only from γ-ray excitation and pulsed-beam γ timing measurements, was different than that expected from an extrapolation of the previous ^{207,209,211}At systematics. The present study used the ^{197}Au (^{12}C,$4n$)^{205}At reaction, but with a more complete set of experiments involving γ-γ coincidence, and γ-ray angular distribution measurements as well as pulsed-beam γ timing. The deduced level scheme from the present study is consistent with the systematics of the ^{207,209,211}At level schemes and is completely different from that of Ref. 7. Preliminary results[8] of the present measurements have been reported previously.

In Sec. II, the techniques for the in-beam γ-ray measurements are briefly described; a more detailed discussion is available in the ^{206}Pb(^{6}Li, $3n$)^{209}At study.[2] The experimental results for ^{205}At are presented in Sec. III and in Sec. IV the level scheme is discussed in terms of the shell model and compared with ^{207,209,211}At.

II. EXPERIMENTAL PROCEDURE

High-spin states in ^{205}At were populated via the ^{197}Au(^{12}C,$4n$) fusion evaporation reaction by bom-

barding a 5 mg/cm^2 ^{197}Au target with 77-MeV ^{12}C ions from the Brookhaven National Laboratory tandem Van de Graaff accelerator. The 77-MeV beam energy was selected on the basis of the earlier ^{197}Au+^{12}C γ-ray excitation measurements,[7] which showed this to be the optimum choice for production of the (^{12}C,4n) channel relative to the 3n and 5n channels. The deexcitation γ rays were detected with large volume Ge(Li) detectors, which typically had energy resolutions of about 2 keV full-width at half-maximum (FWHM) at 1.33 MeV. Three types of experiments were conducted: (1) γ-γ coincidence, (2) γ-ray angular distributions, and (3) pulsed-beam γ timing.

The γ-γ coincidence measurement, which used two Ge(Li) detectors, was carried out in order to identify the detailed γ-ray cascades. The γ-ray angular distributions were measured in singles at five angles between 90° and 160° to provide information regarding the γ-ray multipolarities and spins of the levels, as well as the relative γ-ray intensities I_γ. The angular distribution coefficients A_2 and A_4 were determined by least squares fit to the photopeak areas of the function $W(\theta)=I_\gamma(1+A_2P_2+A_4P_4)$, where the P_k (cosθ) are Legendre polynomials. The photopeak areas were normalized for dead time and geometric effects. Angle normalization was achieved with a fixed angle monitor Ge(Li) detector. The pulsed-beam γ timing measurements were made to determine decay modes of isomeric states and their lifetimes. The beam was pulsed at repetition rates of 1 and 4 μsec with a pulse time width of about 40 nsec FWHM. Both delayed γ-ray spectra for the entire energy range and time differential spectra for specific γ rays were obtained.

III. EXPERIMENTAL RESULTS

Twenty-one γ rays were identified in ^{205}At on the basis of the present ^{197}Au(^{12}C,4n) γ-γ coincidence measurements. These γ rays are labeled in units of keV on the γ-ray singles spectrum at the top of Fig. 1. All the other strong γ rays on this spectrum which are not labeled were identified

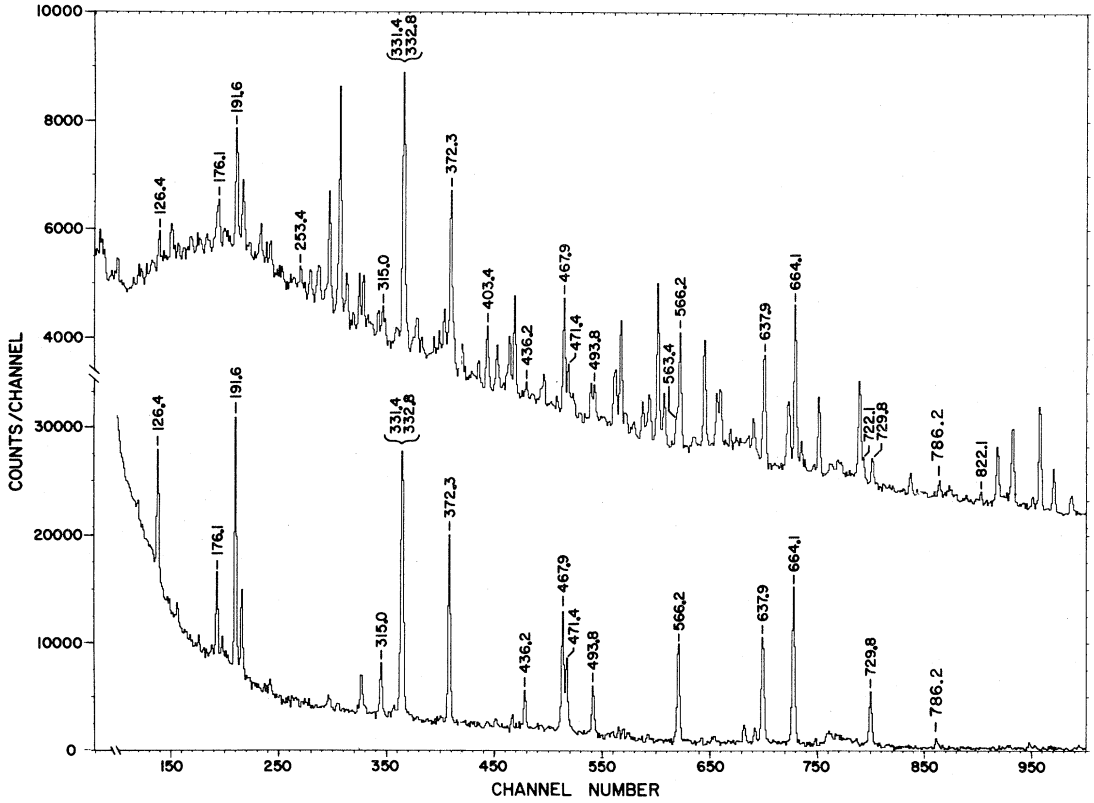

FIG. 1. γ-ray singles and delayed spectra observed with a Ge(Li) detector at 90° to the beam for the bombardment of 5 mg/cm^2 of ^{197}Au with 77-MeV ^{12}C ions. The spectrum on the top is the γ-ray singles. The spectrum on the bottom is the delayed spectrum obtained for a time gate of 50-280 nsec minus a time gate of 340-570 nsec. In this delayed spectrum all the long-lived radioactive γ rays and the 3 μsec component of the 403-keV γ ray are subtracted.

TABLE I. Results of γ-γ coincidence measurements for ^{205}At.

Gate energy (keV)	Coincident γ rays[a]
126.4	332.8, 372.3, 467.9, (566.2), (637.9), 664.1
176.1	331.4, 637.9, 664.1
191.6	467.9, 493.8, 637.9, 664.1, 729.8
253.4	(563.4)
315.0	331.4, 471.4, 637.9
331.4, 332.8[b]	126.4, 176.1, (253.4), 315.0, 372.3, 403.4, (436.2), 467.9, 471.4, 493.8, (563.4), 566.2, 637.9, 664.1, 722.1, 786.2
372.3	126.4, (253.4), 332.8, 403.4, 467.9, 566.2, 637.9, 664.1, 722.1, 822.1
403.4	332.8, 372.3, (403.0), 566.2, 664.1
436.2	(176.1), 331.4, 471.4, 637.9
467.9	191.6, 332.8, 372.3, 664.1, 729.8
471.4	(176.1), 315.0, 331.4, (436.2), 637.9
493.8	191.6, 332.8, 372.3, 637.9, 729.8
563.4	332.8, (664.1)
566.2	126.4, 332.8, 372.3, 403.4, 563.4, 664.1
637.9	(191.6), (315.0), 331.4, 332.8, 372.3, (436.2), 471.4, 493.8
664.1	(126.4), 191.6, (253.4), 332.8, 372.3, 403.4, 467.9, (563.4), 556.2, (722.1), 729.8
722.1	(332.8), 372.3, (637.9), (664.1)
729.8	191.6, 467.9, 493.8, 637.9, 664.1
822.1	(332.8), 372.3, (664.1)

[a]Parentheses around γ-ray energy indicate a weak coincidence.
[b]These two γ rays could not be resolved; however, setting gates in the upper and lower halves of this doublet resulted in significantly different coincident spectra, indicating two different γ rays. For the other γ-ray gates, there was a centroid shift of about three channels between the 331.4- and 332.8-keV γ rays. Thus these two γ rays were separable in most of the coincidence spectra.

with the (^{12}C,3n) and (^{12}C,5n) channels or with radioactive decay. A delayed γ-ray spectrum is at the bottom of Fig. 1.

The results of the γ-γ coincidence measurements are summarized in Table I. With these results a level scheme for ^{205}At was constructed and is shown in Fig. 2. The γ-ray cascades from the 2062-keV level to the ground state represent the main part of this level scheme. The positions of the 176- and 436-keV γ rays in the level scheme are somewhat uncertain. These two weak γ rays of roughly equal intensity are placed, from the γ-γ coincidence results, as a cascade from the 2053-keV level to the 1441-keV level defining a level at 1877 keV. A possible reverse ordering would put the intermediate level at 1617 keV. As will be discussed in Sec. IV, the systematic properties of the At isotopes favor the 1877-keV position.

Two unobserved transitions have also been placed in the ^{205}At level scheme. These are the 98-keV transition between the 1230- and 1132-keV levels and the 9-keV transition between the 2062- and 2053-keV levels. The existence of the 98-keV transition is confirmed by coincidences between the lower-lying 468- and 494-keV γ rays and the higher-lying 333- and 372-keV γ rays. The 9-keV transition is suggested by the pulsed beam γ timing data. This will be discussed below.

All the γ rays listed in Table I, except for the 254-, 563-, and 822-keV γ rays were assigned to the ^{205}At level scheme. The positions of these three γ rays could not be established on the basis of the present experimental coincidence results. None of the γ rays observed[6] in the β decay of ^{205}Rn have been observed in the present experiment.

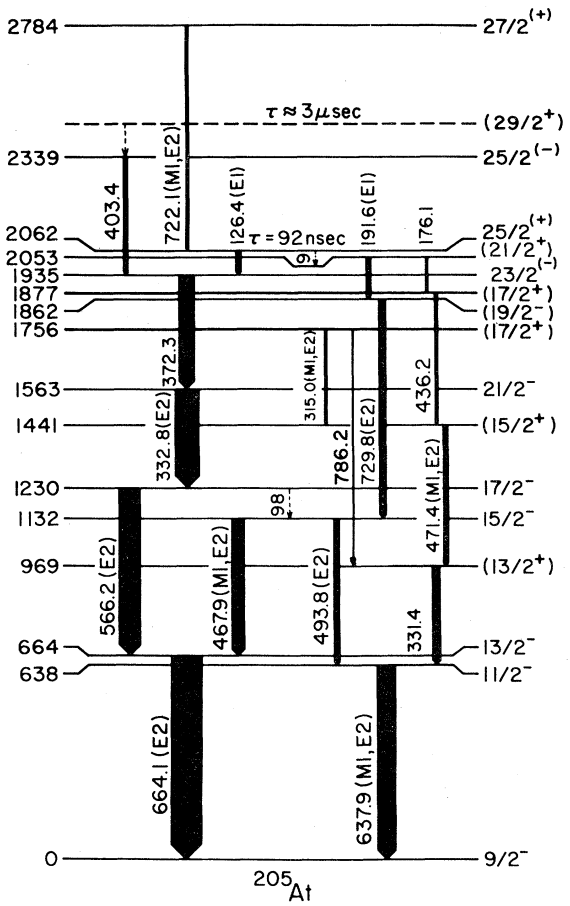

FIG. 2. The energy level scheme for ^{205}At determined from the present ^{197}Au(^{12}C,4n) γ-ray measurements. The energies of the levels and the γ rays are in units of keV. The widths of the arrows are proportional to the observed intensities of the γ rays at a bombarding energy of 77 MeV.

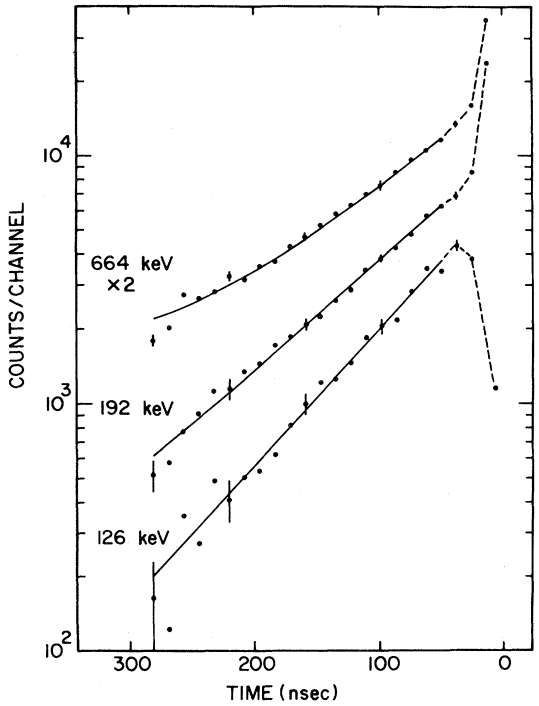

FIG. 3. Results of the time differential lifetime measurement of the 2062-keV $\frac{25}{2}^{(+)}$ state in ^{205}At, obtained from the pulsed beam γ timing spectra of the 126-, 192-, and 664-keV γ rays. The solid lines are least squares fits to the data, which yielded a mean lifetime of $\tau=92(3)$ nsec. The influence of the 3 μsec lifetime can be seen in the time spectrum of 664-keV γ ray.

Evidence for two isomeric states in ^{205}At was found in the pulsed beam γ timing data. From the delayed γ-ray spectra (see Fig. 1), all the γ rays in the ^{205}At level scheme, except for the 722-keV transition, were observed to have delayed components. These delayed components could only be explained by the existence of two isomeric states.

With the time differential measurements, the mean lifetime of these two isomeric states were determined to be $\tau=92(3)$ nsec for the 2062-keV level and $\tau\approx3$ μsec for an unobserved level above 2339 keV. All the γ rays produced in the decay of the 2062-keV level were observed to have the shorter lifetime component. The time spectra for three of these γ rays, the 126-, 192-, and 664-keV transitions, are shown in Fig. 3. Since the time spectrum of the 126-keV γ ray had no prompt component, this indicated that the 2062-keV level was the isomer. The mean lifetime of this isomer was determined from least squares fits to the time spectra for all the γ rays observed in the decay of the 2062-keV level. The weighted average of these fits yielded $\tau=92(2)$ nsec; an uncertainty of ±3 nsec includes possible systematic uncertainties due to the delayed background. The present result is considerably different than the value of $\tau=159(36)$ nsec, which Hagemann *et al.*[7] obtained with their 81-MeV ^{12}C beam. The existence of an unobserved 9-keV transition from the 2062-keV isomer to the 2053-keV level is suggested by the time differential data, since all the γ rays produced in the decay of the 2053-keV level have delayed components with $\tau=92$ nsec.

The long lifetime component was observed in the time spectra of those γ rays produced in the decay of the 2339-keV level. Least squares fits to these data yielded a mean lifetime of $\tau\approx3$ μsec. A more accurate lifetime result was not possible because of the difficulty in defining, with a 4 μsec pulsed

period, the background component for the fitting procedure. The time spectrum for the 403-keV γ ray, which deexcites the 2339-keV level, contained a prompt component after Compton background subtraction. Since no delayed γ rays were observed above this level, this indicated that the long-lived isomer decays via an unobserved, converted transition. For this reason, the $\tau \approx 3$ μsec isomer is denoted by a dotted line above the 2339-keV level in Fig. 2.

Based on the present ^{197}Au(^{12}C,4n)^{205}At time differential measurements, it is not possible to determine whether or not the 192-keV γ ray lacks a prompt peak in its time spectrum. This occurs because the 192-keV γ ray is not resolved from the prompt 191.4-keV transition in ^{197}Au, which is also produced following the bombardment of ^{197}Au with ^{12}C ions. However, according to Hagemann *et al.*,[7] the 192-keV γ ray produced in the ^{193}Ir(^{16}O,4n) ^{205}At reaction has no prompt component. Since the 192-keV γ ray directly decays from the 2053-keV level, this suggests that the level is isomeric itself, and has a lifetime that is not distinguishable (within the present experimental accuracy) from the $\tau = 92$ nsec lifetime of the 2062-keV isomer. If this is true then the deduced 9-keV γ ray need not exist. This possibly is contradicted by the 176-keV transition, which also directly decays from the 2053-keV level and has a prompt component in its time spectrum. On the other hand, since the placement of this γ ray is tentative, the possibility of an isomeric 2053-keV level cannot be ruled out.

The information extracted from the angular distribution measurements is summarized in Table II, where the relative γ-ray intensities and angular distribution A_2 and A_4 coefficients are listed. The deduced J^π assignments for ^{205}At are also included in Table II and in the level scheme in Fig. 2. These assignments were obtained from the angular distribution with the assumptions that the states are aligned in low-m substates and that the dominant γ-ray decay proceeds by stretched transitions $J \rightarrow J - L$, where L refers to the γ-ray multipolarity. These features are expected in (HI,xn) fusion evaporation reactions.[9] Lifetime information and conversion coefficients extracted from the delayed γ-ray intensities also aided in these assignments. The spectroscopic information for the dominant decay cascade shown on the left hand side of Fig. 2 will be discussed first. The population of the levels in this cascade decreases as the energy of the initial state increases. This is characteristic of the population of yrast levels and the subsequent stretched $J \rightarrow J - L$ transitions. The less intense cascade, which is indicative of nonyrast levels, is shown on the right side of the figure.

The large positive A_2 coefficients and lifetime limits identify the 333-, 494-, 566-, and 664-keV γ rays as stretched $J \rightarrow J - 2$ $E2$ transitions, while the large negative A_2 coefficients strongly suggest that the 468-, and 638-keV γ rays are $J \rightarrow J - 1$ $M1/E2$ transitions with negative mixing ratios. Based on an assumed $J^\pi = \frac{9}{2}^-$ for the ground state of ^{205}At, these multipolarities imply the following J^π assignments: 638-keV $\frac{11}{2}^-$, 664-keV $\frac{13}{2}^-$, 1132-keV $\frac{15}{2}^-$, 1230-keV $\frac{17}{2}^-$, and 1563-keV $\frac{21}{2}^-$. For the 372- and 403-keV γ rays, the lifetime limits and A_2 coefficients imply $J \rightarrow J - 1$ stretched dipole transitions. Based on the $\frac{21}{2}^-$ assignment for the 1563-keV level, these multipolarities imply $J = \frac{23}{2}$ and $\frac{25}{2}$ for the 1935- and 2339-keV levels, respectively. From the lifetime information and the systematics of the odd-mass At isotopes (see Fig. 4), the parity of the 1935- and 2339-keV levels is tentatively given as negative. The tentative nature of these assignments is denoted by parentheses. This will be discussed in Sec. IV.

The 126-keV γ ray is identified as an $E1$ transition. The dipole character of this γ ray is implied by the negative A_2 coefficient, while the $E1$ multipolarity is strongly suggested by internal conversion estimates based on the delayed γ-ray intensities for the 126- and 372-keV γ rays. From these intensities it is observed that the 126-keV γ ray undergoes little internal conversion, eliminating the possibility of $M1$. Based on a 1935-keV $\frac{23}{2}^{(-)}$ level, this multipolarity implies $J^\pi = \frac{25}{2}^{(+)}$ for the 2062-keV isomer. For the prompt 722-keV γ ray, the large negative A_2 coefficient is suggestive of a mixed $M1/E2$ multipolarity, which implies $J^\pi = \frac{27}{2}^{(+)}$ for the 2784-keV level.

The 3 μsec mean lifetime measured for the isomer, that is located just above the 2339-keV $\frac{25}{2}^{(-)}$ level, is consistent with a J^π assignment of $(\frac{29}{2}^+)$ for this isomer. A converted $M2$ $(\frac{29}{2}^+ \rightarrow \frac{25}{2}^-)$ is the multipolarity which, for energies ranging up to $\sim$100 keV, provides the appropriate ($\tau = 3$ μsec) transition strength. The total transition strength, being the sum of the γ ray and e^--conversion strengths, is almost independent of energy over 20-100 keV, which corresponds to energies of $\sim$(2360–2440) keV for the $(\frac{29}{2}^+)$ isomer. A transition energy $\gtrsim$100 keV would have a finite detection efficiency via a γ-ray transition. A dis-

TABLE II. Results of the angular distribution measurements for ^{205}At.

E_γ (keV)	I_γ[a]	A_2[b]	$J_i \rightarrow J_f$[c]
126.4±0.3	16	−0.05±0.05	$\frac{25}{2}^{(+)} \rightarrow \frac{23}{2}^{(-)}$
176.1±0.2	11	0.12±0.06	$(\frac{21}{2}^{+}) \rightarrow (\frac{17}{2}^{+})$
191.6±0.4	16[d]		$(\frac{21}{2}^{+}) \rightarrow (\frac{19}{2}^{-})$
253.4±0.3	10	0.46±0.07[e]	
315.0±0.3	10	−0.24±0.06[f]	$(\frac{17}{2}^{+}) \rightarrow (\frac{15}{2}^{+})$
331.4±0.3	~32 [g]		$(\frac{13}{2}^{+}) \rightarrow \frac{11}{2}^{-}$
332.8±0.4	77 [g]	0.29±0.05	$\frac{21}{2}^{-} \rightarrow \frac{17}{2}^{-}$
372.3±0.2	52	−0.18±0.04	$\frac{23}{2}^{(-)} \rightarrow \frac{21}{2}^{-}$
403.4±0.2	20	−0.13±0.03	$\frac{25}{2}^{(-)} \rightarrow \frac{23}{2}^{(-)}$
436.2±0.2	~12[h]		$(\frac{17}{2}^{+}) \rightarrow (\frac{15}{2}^{+})$
467.9±0.2	37	−0.35±0.04	$\frac{15}{2}^{-} \rightarrow \frac{13}{2}^{-}$
471.4±0.4	16	−0.32±0.04	$(\frac{15}{2}^{+}) \rightarrow (\frac{13}{2}^{+})$
493.8±0.3	16	0.31±0.06	$\frac{15}{2}^{-} \rightarrow \frac{11}{2}^{-}$
563.4±0.4	21	0.26±0.08	
566.2±0.2	66	0.28±0.04	$\frac{17}{2}^{-} \rightarrow \frac{13}{2}^{-}$
637.9±0.2	54	−0.36±0.04	$\frac{11}{2}^{-} \rightarrow \frac{9}{2}^{-}$
664.1±0.2	100	0.25±0.04	$\frac{13}{2}^{-} \rightarrow \frac{9}{2}^{-}$
722.1±0.4	10	−0.68±0.06	$\frac{27}{2}^{(+)} \rightarrow \frac{25}{2}^{(+)}$
729.8±0.3	19	0.25±0.05	$(\frac{19}{2}^{-}) \rightarrow \frac{15}{2}^{-}$
786.2±0.4	6	0.25±0.06	$(\frac{17}{2}^{+}) \rightarrow (\frac{13}{2}^{+})$
822.1±0.4	4	−0.37±0.06	

[a] γ-ray intensities are normalized to the 664.1-keV γ-ray yield; intensities are accurate to 10% unless otherwise noted.
[b] Since about 10% of the residual ^{205}At nuclei recoil out of the target, the angular distribution coefficients include a recoil correction for those γ rays with a $\tau = 92$ nsec delayed component; consequently, the errors quoted are larger. The A_4 coefficient is consistent with 0.0 having an uncertainty of about 0.1.
[c] Tentative J^π assignments are denoted by parentheses.
[d] Contaminated by the 191.5-keV transition in ^{197}Au, intensity (accurate to 25%) is estimated from the γ-γ coincidence measurement.
[e] $A_4 = 0.15 \pm 0.11$.
[f] $A_4 = 0.12 \pm 0.10$.
[g] The lower γ ray in this doublet could not be analyzed cleanly, although the A_2 was significantly less than that of the upper γ ray.
[h] Because of background difficulties, the angular distribution for the 436.2 keV γ ray could not be properly extracted. An estimate $I_\gamma \sim 12$ was obtained from the delayed γ-ray spectrum.

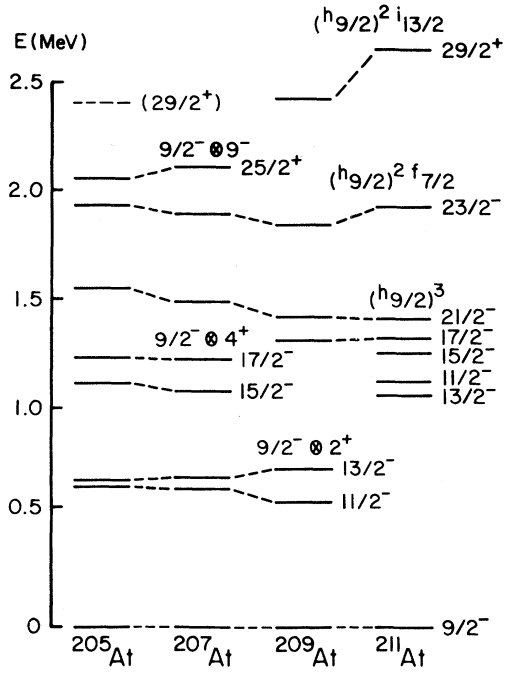

FIG. 4. Yrast levels in ^{205,207,209,211}At. The levels for ^{207,209,211}At were taken from Refs. 1, 2 and 3, respectively.

cussion of competing transitions together with the systematics will be given in Sec. IV.

The remaining γ rays in the ^{205}At level scheme, shown on the right side of Fig. 2, were observed with generally less intensity and appear to involve nonyrast levels. These γ rays, however, are produced in the decay of the $\frac{25}{2}^{(+)}$ level. Since the prompt time spectra restrict these γ rays to dipole or quadrupole multipolarities, it appears that these γ rays also decay via stretched transitions to account for the amount of angular momentum carried away.

Considering the cascade from the 2053-keV level to the 1132-keV level via the 192- and 730-keV γ rays, the large positive $A_2=0.25$ of the 730-keV γ ray suggests an $E2$ multipolarity. This implies a $(\frac{19}{2}^-)$ spin and parity for the 1862-keV level. Although no angular distribution information is available for the 191 keV (it is contaminated by the 191.4-keV γ ray from ^{197}Au), the delayed γ ray intensities strongly suggest an $E1$ multipolarity, which implies $J^\pi=(\frac{21}{2}^+)$ for the 2053-keV level.

For the weak γ cascade from the 2053-keV level to the 638-keV level involving (from the top) the 176-, 436-, 471-, and 331-keV γ rays, only the angular distribution from the 471-keV γ ray could be extracted cleanly; it implies a mixed $M1/E2$ multipolarity. The 331-keV γ ray is part of a doublet; its angular distribution yielded an A_2 coefficient substantially less than that of the stronger 333-keV γ ray which is characteristic of a stretched E2 transition. Because of the lack of a significant lifetime, the properties of the 331-keV transition are then not inconsistent with it being a dipole implying $J=\frac{13}{2}$ for the 969-keV level. As will be discussed later, the feeding and decay transitions for this state along with the At systematics suggest a $(\frac{13}{2}^+)$ assignment for the 969-keV level making the 331-keV γ ray an $E1$ transition. The 471-keV $M1/E2$ γ transition them implies a $J^\pi=(\frac{15}{2}^+)$ for the 1441-keV level. The angular distribution for the 436-keV γ ray could not be obtained, although the 176-keV transition decaying from the $(\frac{21}{2}^+)$ level at 2053 keV is consistent with an $E2$, suggesting a $(\frac{17}{2}^+)$ assignment for the level at 1877 keV.

Finally, the large negative A_2 for the 315-keV γ ray suggests a mixed $M1/E2$ multipolarity and a $J^\pi=(\frac{17}{2}^+)$ for the 1756-keV level. This assignment is corroborated by the weak 786-keV γ ray that is in coincidence with the 332-keV doublet and is in the delayed spectrum; it presumably represents the $E2$ crossover transition to the 969-keV $(\frac{13}{2}^+)$ level which would confirm the 315- and 471-keV transitions as containing $\Delta J=1$, $M1$ components.

The $\frac{25}{2}^{(+)}$ and $(\frac{21}{2}^+)$ spin and parity assignments for the 2062- and 2053-keV levels, respectively, imply that the unobserved 9-keV branch from the $\tau=92$ nsec 2053-keV level is an $E2$ transition. The branching ratio $I[126\text{ keV}]/I[9\text{ keV}]\approx 0.7$ was estimated from the delayed γ-ray intensities. Combining this with an $E2$ internal conversion coefficient estimate[10] of 2.6×10^5 yields $B(E2)\approx 340\ e^2\text{fm}^4$ for the 9-keV branch. This value is enhanced by about a factor of 5 over the Weisskopf estimate.

IV. DISCUSSION

The results of the present ^{197}Au(^{12}C,4n)^{205}At γ-ray measurements are summarized in Tables I and II and in the level scheme of Fig. 2. In the shell model description with ^{208}Pb as a double closed shell nucleus, the ^{205}At levels involve three-proton particle and six-neutron hole configurations of the type $|(\pi)^3 J_p, (\nu)^{-6} J_n, J\rangle$. In Fig. 4, the ^{205}At yrast levels are compared with those of ^{207}At and

^{209}At, which involve $(\nu)^{-4}$ and $(\nu)^{-2}$ neutron configurations, respectively. The yrast levels of the closed neutron shell ($N=126$) ^{211}At, which involve only $|(\pi^3)J\rangle$ configurations relative to ^{208}Pb, are also shown in Fig. 4. These ^{211}At levels are well understood[4] in terms of $(\pi h_{9/2})^3$, $(\pi h_{9/2})^2(\pi f_{7/2})$, and $(\pi h_{9/2})^2(\pi i_{13/2})$ configurations. The systematic comparisons of Fig. 4 show the expected involvement of the various configurations in the yrast-level structure of ^{205}At.

The four lowest lying yrast levels in ^{205}At are the $\frac{11}{2}^-$, $\frac{13}{2}^-$, $\frac{15}{2}^-$, and $\frac{17}{2}^-$ levels at 638-, 664-, 1132-, and 1230-keV, respectively. The large energy reduction of these states relative to the yrast states of corresponding spin parity in ^{211}At suggests that these ^{205}At levels are predominantly the 961-keV 2^+ and 1383-keV 4^+ neutron excitations in ^{202}Pb coupled to the ^{211}At $\frac{9}{2}^-$ ground-state configuration. This energy reduction relative to the ^{211}At yrast levels is also seen for the $\frac{11}{2}^-$, $\frac{13}{2}^-$, $\frac{15}{2}^-$, and $\frac{17}{2}^-$ sequence of levels[1] in ^{207}At and for the $\frac{11}{2}^-$ and $\frac{13}{2}^-$ levels[2] in ^{209}At. Consequently, these states are also identified as being primarily $(\nu)^{-n}J$, $J=2^+$, 4^+ neutron excitations. In ^{209}At, however, no $\frac{15}{2}^-$ yrast level has been observed, and the $\frac{17}{2}^-$ yrast level is identified[2] as the $(\pi h_{9/2})^3$ $\frac{17}{2}^-$ proton excitation coupled to the ^{206}Pb core. This $\frac{17}{2}^-$ proton excitation is yrast in ^{209}At, because the 4^+ state in ^{206}Pb lies 300–400 keV higher than those in ^{202}Pb and ^{204}Pb. The $\frac{15}{2}^-$, $\frac{17}{2}^-$ proton excitations lie higher in energy than the neutron excitations in ^{205,207}At.

The comparison in Fig. 4 strongly suggests that the 1563-keV $\frac{21}{2}^-$ and 1935-keV $\frac{23}{2}^-$ levels in ^{205}At, as in ^{207,209}At, are predominantly $(\pi h_{9/2})^3$ $\frac{21}{2}^-$ and $(\pi h_{9/2})^2(\pi f_{7/2})\frac{23}{2}^-$ protons excitations coupled to the ^{202}Pb ground state $(\nu)^{-6}0^+$. The yrast systematics in Fig. 4 show that the $\frac{21}{2}^-$ and $\frac{23}{2}^-$ levels are increasing in energy relative to the ground state as the number of neutron holes increases. This feature is also observed in the even-Po (Ref. 11) and Rn (Ref. 12) isotopes for the 8^+ and 6^+ levels, which are known to contain $\pi(h_{9/2})^2J$ configurations.

Comparison of the properties of the $\frac{25}{2}^+$ isomer in ^{205}At with those measured earlier[1] for the $\frac{25}{2}^+$ isomer in ^{207}At shows that the two states are very similar. Both states have nearly equal excitation energies of 2062 keV in ^{205}At vs 2117 keV in ^{207}At; both states are isomeric with similar mean lifetimes of 92 nsec in ^{205}At vs 156 nsec in ^{207}At; and both states decay to $\frac{23}{2}^-$ levels via severely hindered $E1$ transitions with $B(E1)$ values of 2.68×10^{-6} e^2fm^2 in ^{205}At vs 3.57×10^{-7} e^2fm^2 in ^{207}At. [The ^{205}At $B(E1)$ value was obtained with an internal conversion coefficient[10] of 0.261 for the 126-keV γ ray.] The $B(E1)$ values are hindered by about factors of 10^7 relative to the Weisskopf estimates. These similarities imply that the $\frac{25}{2}^+$ isomer in ^{205}At has the same structure as the ^{207}At $\frac{25}{2}^+$ isomer, which has been identified by a g-factor measurement[1] to be a $(\nu f_{5/2})^{-1}(\nu i_{13/2})^{-1}$ 9^- neutron quasiparticle excitation coupled to the ^{211}At $\frac{9}{2}^-$ ground state. The similar energies of the $\frac{25}{2}^+$ isomers in ^{207,205}At can easily be understood, since the 9^- states in ^{204}Pb and ^{202}Pb are at 2186 and 2170 keV, respectively. The interpretation of the ^{205}At $\frac{25}{2}^+$ isomer and the $\frac{23}{2}^-$ level as predominantly $|(\pi h_{9/2})^3\frac{9}{2}^-, (\nu f_{5/2})^{-1}$ $\times(\nu i_{13/2})^{-1}$ $9^-, \frac{25}{2}^+\rangle$ and $|(\pi h_{9/2})^2(\pi f_{7/2})\frac{23}{2}^-,$ $(\nu)^{-6}$ $0^+, \frac{23}{2}^-\rangle$ configurations is also consistent with the severely hindered $\frac{25}{2}^+\rightarrow\frac{23}{2}^-$ $E1$ transition, because a single particle transition between these two pure configurations is forbidden.

The isomeric nature of the $\frac{25}{2}^+$ yrast state exhibits the interesting feature that it is the lowest member of the $|(\pi h_{9/2})^3\frac{9}{2}^-, (\nu i_{13/2})^{-1}$ $\times(\nu f_{5/2})^{-1}9^-;J\rangle$ multiplet, which has a maximum spin $J_{\max}=\frac{27}{2}^+$. The observation agrees with the semiempirical $J_{\max}-1$ rule,[13] which predicts that the lowest lying member of a $|(\pi)J_p, (\nu)^{-2}J_n;J\rangle$ three quasiparticle multiplet will have a spin $J=J_{\max}-1$. The observation of this feature in the At isotopes suggest the $J_{\max}-1$ rule, which arises from the neutron-hole, proton-particle effective interaction, is also valid for $|(\pi)^3J_p, (\nu)^{-2}J_n;J\rangle$ multiplets involving predominantly seniority-one $(\pi)^3$ configurations. A shell model calculation[1] of the energies for this multiplet was able to reproduce the $J_{\max}-1$ feature and show that it occurs because the j dependence of the $\langle J_p,J_n^{-1};j\,|\,V_{12}\,|\,J_p,J_n^{-1};j\rangle$ particle-hole matrix elements is relatively weak except for maximum and minimum spin j. For the extreme spins, the matrix elements are enhanced considerably, becoming more repulsive. Thus the $J_{\max}=\frac{27}{2}^+$ member of the multiplet is pushed up $\sim$500 keV in the calculation above the $\frac{25}{2}^+$ state. The $\frac{27}{2}^{(+)}$ level at 2784 keV in ^{205}At is possibly this $J_{\max}$ member. The $J_{\max}-1$ rule also appears to be valid for those yrast states in ^{205,207,209}At which are identified as $(\nu)^{-n}J$, $J=2^+$, 4^+ Pb core excitations coupled to the ^{211}At ground state.

The $\tau=3$ μsec isomer at an energy of

$\sim$(2360−2440) keV in ^{205}At is expected to be the $(\pi h_{9/2})^2(\pi i_{13/2})\frac{29}{2}^+$ proton excitation. The energy is consistent with those for the corresponding $\frac{29}{2}^+$ states in ^{209,211}At as shown in Fig. 4. The $\frac{29}{2}^+$ state was not observed in ^{207}At presumably because of limitations of the ^{204}Pb (^{6}Li,$3n\gamma$)^{207}At reaction at 34 MeV.[1] In ^{209}At, the $\frac{29}{2}^+$ state decays via a 577-keV $E3$ transition to the $(\pi h_{9/2})^2\,(\pi f_{7/2})\frac{23}{2}^-$ state with a mean lifetime of $\tau=980$ nsec.[2] The corresponding $E3$ decay transition in ^{205}At would yield a $\tau \gtrsim 6$ μsec because of the reduced transition energy, and thus does not compete with an $M2$ transition to the $\frac{25}{2}^{(-)}$ state at 2339 keV. An $E2$ transition from the $(\frac{29}{2}^+)$ proton excitation to the $\frac{25}{2}^{(+)}$ neutron excitation, which was not observed, is obviously strongly hindered. This is consistent with rather pure configurations, for which the γ-ray transition would be forbidden.

Dominant configurations are also suggested by the systematics for several of the nonyrast states of the ^{205}At level scheme. The $(\frac{21}{2}^+)$ level at 2053 keV, which is only 9 keV lower in energy than the $\frac{25}{2}^+$ isomer, most probably involves the $|(\pi h_{9/2})^3\frac{9}{2}^-(\nu)^{-6}\,7^-;\frac{21}{2}^+\rangle$ configuration. This is suggested because the 2208-keV 7^- level in ^{202}Pb is very similar in energy to the $\frac{21}{2}^+$ level. Moreover, the only other possible $\frac{21}{2}^+$ state involves the $|(\pi h_{9/2})^3\frac{9}{2}^-, (\nu i_{13/2})^{-1}(\nu f_{5/2})^{-1}\,9^-;J\rangle$ multiplet and is expected to lie above the 2062-keV $\frac{25}{2}^+$ state (see Ref. 1). The unobserved 9 keV $E2$ transition between the $\frac{25}{2}^{(+)}$ and $(\frac{21}{2}^+)$ levels, which is enhanced by about 5 W.u., is not inconsistent with the suggested configuration.

For the $(\frac{19}{2}^-)$ level at 1862 keV in ^{205}At, the $|(\pi h_{9/2})^2(\pi f_{7/2})\frac{19}{2}^-\,(\nu)^{-6}\,0^+;\frac{19}{2}^-\rangle$ configuration is most likely the dominant component. The structure differences between this $\frac{19}{2}^-$ level and the 2053-keV $\frac{21}{2}^+$ level implies that the 191-keV $E1$ transition should be hindered on the same order as the $E1$ transition between the $\frac{25}{2}^+$ and $\frac{23}{2}^-$ levels. If $B(E1)[\frac{21}{2}^+\rightarrow\frac{19}{2}^-]\approx B(E1)[\frac{25}{2}^+\rightarrow\frac{23}{2}^-]$, then the mean lifetime of the 2053-keV $(\frac{21}{2}^+)$ level would be about 26 nsec. A lifetime for this level on the order of $\tau\lesssim 92$ nsec is not inconsistent with the possible isomerism of the $(\frac{21}{2}^+)$ 2053-keV level as discussed in Sec. III.

Finally, the states that cascade decay to the 969-keV $(\frac{13}{2}^+)$ level do not have any significant decay branch to the negative parity levels involving the $(\pi h_{9/2})^3$ configuration. This feature has been recently observed[14] for ^{201,203}At for which the corresponding $\frac{13}{2}^+$ assignment is more definite, and also possibly in ^{207}At for the 1116 keV level assigned[1] $(\frac{13}{2})$. These $(\frac{13}{2}^+)$ levels, which consistently drop in energy as A decreases, presumably can be identified with the $|(\pi h_{9/2})^2\,0^+, \pi i_{13/2};\frac{13}{2}^+\rangle$ proton configuration coupled to the 0^+ ground state of the Pb cores. The $(\frac{15}{2}^+)$ and $(\frac{17}{2}^+)$ levels in ^{205}At at 1441 and 1756 keV, respectively, which cascade decay to the 969-keV $(\frac{13}{2}^+)$ level, are most probably this $\pi i_{13/2}$ configuration coupled to the $(\nu)^{-2}2^+$ core with $J_{\max}-1$ the lowest. Transitions from these positive parity configurations to the negative parity levels would be strongly hindered.

An additional $\frac{17}{2}^+$ state is expected just below the $\frac{25}{2}^+$ level from the $J_{\max}-1$ member of the $|(\pi h_{9/2})^3\frac{9}{2}^-;(\nu)^{-2}5^-;J\rangle$ configuration in ^{205}At. The 5^- level in ^{202}Pb is 129-keV lower than the 9^- level which suggests that the 1877-keV $(\frac{17}{2}^+)$ level in ^{205}At is a good candidate for this configuration. The 1877-keV level is fed by the 2053-keV $(\frac{21}{2}^+)$ level via the 176-keV γ ray, which would then be equivalent to the $7^-\rightarrow 5^-$ ^{202}Pb core transition.

The most striking feature in the comparison of the ^{205,207,209,211}At yrast levels in Fig. 4 is that the yrast level schemes for ^{205}At and ^{207}At are nearly identical, both being somewhat different from ^{209}At. In contrast, the ^{209}At yrast level scheme bears a closer resemblence to ^{211}At than do those of ^{205,207}At. This can be understood qualitatively, since both the ^{202}Pb and ^{204}Pb yrast level schemes are nearly identical, while that for ^{206}Pb is somewhat different, with the yrast 4^+ and 9^- levels being considerably higher in energy than in ^{202,204}Pb. Thus, because the 4^+ and 9^- levels are lower in ^{202,204}Pb, the neutron-hole excitations are more involved in the yrast structure of ^{205,207}At. The strong influence of the Pb excitations is also evident in ^{213}At,[3] where the low-lying yrast levels are observed to involve the $(\nu)^2$ excitations of ^{210}Pb. As can be seen in Figs. 2 and 4, no significant collectivity in terms of band structure has developed at these excitation energies in the At isotopes down to $N=120$.

This study was supported in part by the National Science Foundation and by the Department of Energy.

*Present address: Oak Ridge National Laboratory, Oak Ridge, Tennessee 37830.
†Present address: Cyclotron Institute, Texas A&M University, College Station, Texas 77843.
‡Present address: Institut fur Kernphysik, Kernsforschungsenlage Julich, D-5179 Julich, West Germany.
§Permanent address: Physics Dept., University of Auckland, Auckland, New Zealand.

[1]T. P. Sjoreen, U. Garg, and D. B. Fossan, Phys. Rev. C 23, 272 (1981); Phys. Lett. 76B, 397 (1978).
[2]T. P. Sjoreen, G. Schatz, S. K. Bhattacherjee, B. A. Brown, D. B. Fossan, and P. M. S. Lesser, Phys. Rev. C 14, 1023 (1976).
[3]T. P. Sjoreen, U. Garg, and D. B. Fossan, Phys. Rev. C 21, 1838 (1980).
[4]H. Ingwersen, W. Klinger, G. Schatz, and K. Witthuhn, Phys. Rev. C 11, 243 (1975).
[5]M. Pautrat, G. Albouy, J. C. David, J. M. Lagrange, N. Poffé, C. Roulet, H. Sergolle, J. Vanhorenbeeck, and H. Abou-Leila, Nucl. Phys. A201, 449, (1973); A201, 469 (1973).
[6]M. R. Schmorak, Nucl. Data Sheets 23, 287 (1978).
[7]U. Hagemann, W. Neubert, W. Schulze, and F. Stary, Nucl. Phys. A181, 145 (1972).
[8]T. P. Sjoreen, D. B. Fossan, U. Garg, A. Neskakis, A. R. Poletti, and E. K. Warburton, Proceedings of the International Symposium on High-Spin Phenomena in Nuclei, Argonne, 1979, Argonne National Laboratory Report ANL/PHY-79-4, 1979, p. 469.
[9]J. O. Newton, in *Nuclear Spectroscopy and Reactions,* edited by J. Cerny (Academic, New York, 1974), p. 185.
[10]R. S. Hager and C. E. Seltzer, Nucl. Data A4, 1 (1968); O. Dragoun, Z. Plajner, and F. Schmutzler, *ibid.* A9, 119 (1971).
[11]H. Beuscher, D. R. Zolnowski, D. R. Haenni, and T. T. Sugihara, Phys. Rev. Lett. 36, 1128 (1976); K. Wikström, I. Bergström, J. Blomqvist, and C. J. Herrlander, Phys. Scr. 10, 292 (1974).
[12]A. R. Poletti, G. D. Dracoulis, and C. Fahlander, Phys. Rev. Lett. 45, 1475 (1980).
[13]L. K. Peker, Yad. Fiz. 4, 27 (1966) [Sov. J. Nucl. Phys. 4, 20 (1967)]; J. Nucl. Phys. (USSR) 4, 27 (1966).
[14]K. Dybdal, T. Chapuran, D. B. Fossan, W. F. Piel, Jr., D. Horn, and E. K. Warburton, Bull. Am. Phys. Soc. 26, 621 (1981).